Direct Synthesis of Aqueous CdSe/ZnS-Based Quantum Dots Using Microwave Irradiation

William Schumacher, Amber Nagy, W. James Waldman, and Prabir K. Dutta*

Departments of Chemistry and Pathology, The Ohio State University, Columbus, Ohio 43210

Received: February 3, 2009; Revised Manuscript Received: May 19, 2009

This study focuses on an aqueous one-pot method for synthesis of CdSe/ZnS core/shell QDs using microwave radiation. The novelty of the study is the use of $Zn(NH_3)_4^{2+}$ as the zinc source. Using an initial solution with the composition $Cd_1Se_1Zn_6MPA_{20}$, the QDs obtained upon heating at 160 °C for 60 min were not high quality, as evidenced by a quantum yield of 1.5%, due to the poor interface between the core and shell. Postsynthesis UV irradiation of the as-prepared QDs for 30 min could be used to improve the quantum yield to 22%, but the technique is not practical for large-scale applications. By increasing the amount of Cd^{2+} in the initial solution to $Cd_4Se_1Zn_4MPA_{20}$, we formed CdSe/CdS/ZnS QDs after heating at 150 °C for 90 min, which contained less interfacial trap-states and as a result, had a higher quantum yield of 13%. These QDs were characterized by powder diffraction, electron microscopy, and X-ray photoelectron spectroscopy. Uptake of the microwave-optimized QDs by alveolar macrophages was compared in a side-by-side study against commercial QDs, QDot585. Despite having a lower relative quantum yield (13%) as compared to the commercial QDs (65%), the microwave-synthesized QDs at 20 nM concentrations were readily detected within the macrophages after 20 min of incubation.

Introduction

Semiconductor nanocrystals known as quantum dots (QDs) are in high-demand as inorganic fluorophores.[1,2] Compared to traditional organic fluorophores, they offer several advantages, including flexible photoexcitation, sharp photoemission, and superb resistance to photobleaching.[3,4] Additionally, by changing the size or composition of the nanocrystals, their optical properties can be tailored to meet specific wavelength requirements.[5] Recent advances in bioconjugation techniques have increased the use of QDs as biological labeling agents, and numerous examples documenting success are present in the literature.[1−3] However, the relatively high cost of commercial QDs is a limiting aspect to their widespread use. In response, there is a need to develop simple, low-cost methods for generating high-quality QDs that can be used as biological labeling agents.

Since the inception of QDs in the early 1980s, a multitude of synthetic methods have been proposed. A major breakthrough occurred in 1993 when Murray et al. identified dimethyl cadmium, $Cd(CH_3)_2$, as a precursor for synthesizing QDs in organic medium at high temperatures.[6] The resulting nanocrystals possessed outstanding crystallinity and high quantum yields but required the use of toxic and pyrophoric precursors at elevated temperatures. A noteworthy improvement to that method was the incorporation of the less reactive cadmium oxide precursor, CdO,[7] but this approach, too, had a shortcoming; organic-derived QDs were not easily dispersed in water without undergoing a significant loss in quantum yield.[8] Alternatively, aqueous-derived QDs are suitable for biological studies as-prepared, and the synthetic methods are generally safer, simpler, and less expensive. Using a metal salt and NaHE (E = Se, Te, etc.), Kapitonov et al. and Rogach et al. synthesized thiol-stabilized CdTe QDs and CdSe QDs, respectively.[9,10] However, aqueous-based QDs typically took hours or days to prepare[11] and they usually possessed poor crystallinity and quantum yields below 10%.[12]

The notion of using microwave electromagnetic irradiation to synthesize QDs is gaining in popularity because it can provide rate and yield enhancements, as well as scalability.[13] These benefits can be explained by dielectric heating in which polar materials are heated preferentially because they absorb microwaves more strongly. Depending on the relative polarity difference between the solvent and precursor molecules, one can rapidly grow QDs by heating precursors directly or by heating the solvent to form a traditional thermal bath. Furthermore, dielectric heating differs from convective heating in that the entire volume is heated uniformly, thereby reducing thermal gradient effects and hence providing more control over the size distribution (i.e., optical properties) of the QDs.[13] Therefore, with careful selection of the reaction system (precursors, passivating ligands, solvent, etc.) and microwave parameters (temperature, time, power, etc.), one can potentially achieve superior control of the nucleation and growth processes to generate high-quality QDs.

Ren et al. used microwave irradiation to prepare water-soluble CdTe QDs with high quantum yields (40−60%) in as little as five minutes.[14] This work was later modified by Qian et al. to tailor methods for CdSe(S) and ZnSe(S) QDs.[15,16] Qian et al. used a ligand, 3-mercaptopropionic acid (MPA), which not only passivated the QDs but also served as the S^{2-} source at high reaction temperatures. To make CdSe(S) QDs, CdSe initial nanocrystals were first nucleated by rapid addition of sodium hydrogen selenide, NaHSe, to an aqueous solution containing Cd^{2+} ions and MPA. At reaction temperatures below 120 °C, the CdSe nanocrystals grew and crystallized while the MPA merely passivated the QDs. At temperatures above 120 °C, a fraction of the MPA ligands decomposed to release S^{2-} ions, which then reacted with excess Cd^{2+} to form CdSe(S) gradient alloy QDs. While these QDs had good crystallinity and a quantum yield reaching 25%, they may be of limited use to biological labeling. Namely, the thick CdS shell can be excited

* To whom correspondence should be addressed. E-mail: dutta@chemistry.ohio-state.edu.

10.1021/jp901003r CCC: $40.75
Published on Web 06/19/2009

by UV light and evidence also suggests that Cd^{2+}-rich QD surfaces are toxic.[17,18] Very recently, He et al. developed an aqueous microwave-assisted route for synthesizing CdTe/CdS/ZnS core−shell−shell QDs that had good photostability and biocompatibility because of the outermost ZnS shell.[19] However, this method used separate growth and purification steps for each component (core−shell−shell), and a single step method would be more optimum and was the goal of this study.

We investigated a one-pot scheme for the direct synthesis of aqueous CdSe/ZnS QDs using microwave irradiation. Compared to CdS, formation of a ZnS shell should provide more passivation of the CdSe core (since $E_{gZnS} > E_{gCdS}$) and reduce the probability of dual-excitation and toxicity. Our approach is based on the addition of a water-soluble Zn^{2+} complex, $Zn(NH_3)_4^{2+}$, to a solution containing CdSe initial nanocrystals and MPA. We show that subsequent microwave heating of these initial solutions for less than 2 h can result in high-quality CdSe/ZnS-based QDs possessing good photoluminescent quantum yield (QY) and biocompatibility.

Experimental Section

Chemicals. Cadmium chloride hemipentahydrate, $CdCl_2 \cdot 2.5\ H_2O$ (≥98%), and sodium borohydride, $NaBH_4$ (99%), were obtained from Aldrich (Milwaukee, WI). Zinc chloride, $ZnCl_2$ (99.99%), MPA, and Se powder (>99.5%, 200 mesh) were obtained from Acros (Geel, Belgium). Sodium hydroxide, NaOH, and ammonium hydroxide, NH_4OH (28−30%), were obtained from Mallinckrodt Chemicals (Phillipsburg, NJ). All chemicals were used without further purification. The H_2O used in this study was purified by a Barnstead NANOpure Infinity ultrapure water system (Dubuque, IA).

Precursor Solutions. ***Cd-MPA Stock.*** A specified volume of a 5.0 mM $CdCl_2 \cdot 2.5\ H_2O$ stock solution was mixed with MPA in H_2O, and the pH of the solution was adjusted to 9.5 by using 1 M NaOH. The Cd^{2+} concentration of the Cd-MPA stock solution ranged from 0.263−1.84 mM, while the MPA concentration was held constant at 5.26 mM. The optically transparent solution was protected from light and stored at room temperature until needed.

NaHSe Stock. The method for preparation of NaHSe has been described elsewhere.[20] Briefly, 152 mg (4 mmol) of $NaBH_4$ was transferred to a vial and cooled to 0 °C at which time 2.0 mL of H_2O and then 158 mg (2 mmol) of Se powder were added. The contents of the vial were immediately sealed and continually flushed with N_2 gas. An outlet was inserted through the seal to release pressure from the flowing N_2 gas and H_2 gas evolved during the reaction. After approximately 30 min of intense bubbling, the black Se powder disappeared and a white $Na_2B_4O_7$ precipitate formed. After 3 h, an aliquot of the clear NaHSe supernatant was transferred to a sealed flask containing N_2-saturated H_2O to make a 20 mM NaHSe stock solution. NaHSe must be prepared immediately before use.

$Zn(NH_3)_4^{2+}$ Stock. A 60 mM $Zn(NH_3)_4^{2+}$ stock solution was prepared by dissolving $ZnCl_2$ in H_2O and titrating with NH_4OH. Initially upon adding NH_4OH, a white $Zn(OH)_2$ precipitate formed that eventually dissolved by pH 10.5 to form the $Zn(NH_3)_4^{2+}$ complex. The optically transparent solution was protected from light and stored at room temperature until needed. For studies that required more than one day of testing, the solution was stored at 4 °C.

$Cd_xSe_1MPA_{20}$/$Cd_xSe_1Zn_yMPA_{20}$ Initial Solutions and Microwave Irradiation. A 250 μL volume of NaHSe stock solution was swiftly injected into 19.0 mL of the Cd-MPA solution under vigorous stirring and ambient conditions to nucleate CdSe initial nanocrystals. After one hour, 750 μL of H_2O (for $Cd_xSe_1MPA_{20}$; $x = 1-7$) or 750 μL of $Zn(NH_3)_4^{2+}$ diluted from the stock solution (for $Cd_xSe_1Zn_yMPA_{20}$; $x = 1-7$, $y = 1-7$) was added to the initial solution and the contents (final volume = 20.0 mL) were sealed in a digestion vessel and subjected to microwave irradiation (MARS5 microwave system, CEM Corp.). Microwave experiments were conducted at 300 W using programmed temperature gradients that typically ranged between 140−170 °C and 45−120 min. For all experiments, the final NaHSe and MPA concentrations remained fixed at 0.25 and 5.0 mM, respectively. For convenience, we are reporting the reactant composition normalized to the molar ratios of the Se^{2-} concentration (0.25 mM = 1 mol equiv).

Characterization Techniques. Aliquots (250 μL) of the as-prepared QD solutions were diluted to 2.5 mL with H_2O for optical measurements. UV−vis absorption spectra were measured with a Shimadzu UV-2501PC UV−vis recording spectrophotometer and photoluminescence (PL) spectra were collected with a Spex Fluorolog 0.22-m double spectrometer (excitation at 375 nm). All optical measurements were carried out at room temperature. QY measurements were estimated by comparison to the photoluminescence intensity of rhodamine 6G with the same absorbance, 0.02 A.U., at 480 nm excitation (QY = 95%).

High resolution transmission electron microscopy (HRTEM) images of the as-prepared QDs were obtained by using a Tecnai-F20 system with an acceleration voltage of 200 kV. The QDs were deposited from a dilute solution onto a non-Formvar copper grid with an ultrathin carbon film on a holey carbon support film. Size determinations were made by analyzing the diameter of at least 50 QDs.

As-prepared QD solutions were purified by precipitation with 2-propanol then dialyzed extensively into H_2O and dried overnight in a vacuum oven. X-ray diffraction (XRD) powder spectra were recorded using a Bruker D8-advance system equipped with nickel-filtered Cu Kα radiation (1.5405 Å). X-ray photoelectron spectroscopy (XPS) surface analysis was carried out using a Kratos Axis Ultra system equipped with monochromated Al radiation (1486.6 eV). All binding energies were calibrated with respect to the C 1s line at 285 eV and then normalized to the Se 3d peak to estimate the molar ratio of elements in the product. The S 2p peak was not used in this calculation because its peak area overlapped with the Se 3p peak area.

Dynamic light scattering (DLS) was used to monitor the size of the QDs. A Brookhaven Instruments 9000 digital correlator with detector positioned at 90° from the incident laser was employed. The Coherent Innova 90c argon ion laser was operated at 200 mW at a wavelength of 514.5 nm. The exponential sampling algorithm was used to calculate particle size.

Post-Synthesis UV Illumination. Aliquots (250 μL) of the as-prepared QD solutions were diluted to 2.5 mL with H_2O and subjected to UV irradiation using a 150 W Xe lamp (model UXL151HXE, PTI) at ambient temperature while being stirred. The solutions were placed in the same position relative to the lamp to ensure equal spatial distribution of the energy throughout the irradiation process. The radiation energy from the lamp through a 350−450 nm dichroic filter and water filter to the solution was measured as 225 mW cm^{-2}. Also, the solution cuvettes were sealed with parafilm to prevent sample loss due to evaporation. Optical measurements were performed on the resulting solutions without any modification.

TABLE 1: Effect of [Zn^{2+}] and Microwave Heating Temperature (Heated for 60 Minutes) on QDs from $Cd_1Se_1Zn_yMPA_{20}$ Initial Solution[a]

Cd/Se/Zn/MPA	temperature	λ_{maxQD}	I_{maxQD}	I_{maxTS}	I_{maxQD}/I_{maxTS}
1:1:0:20	140 °C	616 nm	1.7×10^4	1.6×10^5	0.1
1:1:1:20	140 °C	545 nm	6.2×10^4	8.4×10^5	0.1
1:1:2:20	140 °C	567 nm	5.0×10^5	1.9×10^6	0.3
1:1:3:20	140 °C	567 nm	1.2×10^6	2.3×10^6	0.5
1:1:4:20	140 °C	567 nm	2.4×10^6	2.8×10^6	0.9
1:1:5:20	140 °C	568 nm	3.9×10^6	2.9×10^6	1.3
1:1:6:20	140 °C	569 nm	5.5×10^6	2.9×10^6	1.9
1:1:6:20	150 °C	574 nm	5.1×10^6	1.9×10^6	2.7
1:1:6:20	160 °C	576 nm	3.6×10^6	1.0×10^6	3.6
1:1:6:20	170 °C*				

[a] QD solutions were excited at 375 nm (* precipitate formed at 170 °C). Cd/Se/Zn/MPA = molar ratio used in initial QD solution; temperature = microwave reaction temperature; $\lambda_{ma\ QD}$ = PL peak QD wavelength; I_{maxQD} = PL peak QD wavelength intensity; I_{maxTS} = peak intensity of QD trap-state emission.

Cell Culture and Biological Imaging. Murine alveolar macrophages were purchased from American type Culture Collection. Cells were cultured with RPMI-1640 media (Gibco) and supplemented with 10% fetal bovine serum (Atlanta Biologicals) and 0.1% penicillin-streptomycin (Gibco). Cells were propagated in T-162 flasks (Corning) and passaged every 3−4 days. For experimentation, cells were removed from the culture flasks using a 0.25% trypsin/EDTA solution (Invitrogen) and initiated into 8-chamber slides (Nalge Nunc) at a density of 2×10^4 cells/chamber. Cells were allowed to adhere to the slides for 24 h prior to QD exposure.

Microwave-synthesized QDs were applied to macrophages grown on 8-chamber slides using serially diluted suspensions ranging from 500 to 4 nM. For comparison, commercial Qdot585 ITK QDs (Invitrogen) were also applied at the same concentrations. Untreated cells served as the negative control. The slides incubated for 20 min to one hour at 37 °C and 5% CO_2. Slide chambers were removed before rinsing with PBS to eliminate uninternalized QDs. Cells were then permeabilized and fixed with 99.5% reagent grade acetone (Sigma) at 4 °C for ten minutes.[21] Finally, slides were air-dried and mounted with coverslips after adding Prolong Gold antifade mounting media containing DAPI (Invitrogen). Slides were viewed on a Zeiss 510 Meta laser scanning confocal microscope. Both types of QDs were excited at 488 nm using an argon laser. DAPI was excited at 360 nm. The color of the quantum dots was chosen to be red to enhance visibility of potential colocalization.

Results

Our experimental strategy involved microwave irradiation of colloidal CdSe in the presence of a Zn^{2+} and S^{2-} source. By controlling the concentrations of Cd^{2+} and Zn^{2+} in the initial solution, as well as the microwave heating parameters, we modified the physical and optical properties of the resulting QDs. In two cases, the QDs were isolated and characterized.

$Cd_1Se_1Zn_yMPA_{20}$ Initial Solution. An initial solution containing one molar equivalent of both Cd^{2+} and Se^{2-} was examined. Different concentrations of the $Zn(NH_3)_4^{2+}$ complex were added to make $Cd_1Se_1Zn_yMPA_{20}$ solutions and the contents were heated in the microwave oven at 140 °C for 60 min. The resulting solutions were stable for months and ranged in color from brown ($y = 0$) to yellow ($y = 1$) to light orange ($y = 2-6$). Photoluminescence (PL) spectra of these solutions were collected and summarized in Table 1. In particular, the PL peak wavelength (λ_{maxQD}) and intensity (I_{maxQD}) corresponding to the QD band-edge emission, and the peak intensity of the trap-state (TS) emission (broad, typically 600−850 nm, I_{maxTS}) were used to describe the solutions. At the lowest Zn^{2+} concentration ($y = 1$), we observed a significant blue shift in λ_{maxQD} when comparing to the analogous sample without Zn^{2+} (616 nm → 545 nm). Additionally, I_{maxQD} and I_{maxTS} increased by 3-fold and 5-fold, respectively. On adding an excess of Zn^{2+} ($y = 6$), λ_{maxQD} stabilized around 569 nm while I_{maxQD} and I_{maxTS} increased by 323-fold and 18-fold, respectively. The brightest QD solutions (relative QY ≈ 2.0%, fwhm = 40 nm), which also possessed the highest I_{maxQD}/I_{maxTS} ratio, 1.9, were prepared from a $Cd_1Se_1Zn_6MPA_{20}$ initial solution. We also studied the effects of microwave heating temperature on the $Cd_1Se_1Zn_6MPA_{20}$ solution (Table 1). By increasing the microwave reaction temperature from 140 to 160 °C, λ_{maxQD} red shifted from 569 to 576 nm and I_{maxQD} and I_{maxTS} dropped 35 and 65%, respectively. At 170 °C, a precipitate was formed during microwave irradiation. Thus, the highest I_{maxQD}/I_{maxTS} ratio from the $Cd_1Se_1Zn_6MPA_{20}$ initial solution was achieved by heating at 160 °C for 60 min (I_{maxQD}/I_{maxTS} ratio = 3.6, relative QY ≈ 1.5%, fwhm = 44 nm).

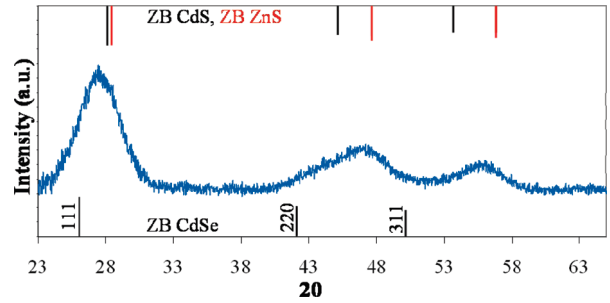

Figure 1. Powder X-ray diffraction pattern of the QDs prepared by heating a $Cd_1Se_1Zn_6MPA_{20}$ initial solution at 160 °C for 60 min. For comparison, the standard diffraction lines for zinc-blende CdSe (below), zinc-blende CdS (above), and zinc-blende ZnS (above, red) are also shown.

We isolated and characterized the QDs prepared by heating a $Cd_1Se_1Zn_6MPA_{20}$ initial solution at 160 °C for 60 min. Figure 1 shows the XRD pattern, which is typified by three broad peaks in the 20−60° 2θ range that matched most closely the zinc-blende ZnS diffraction pattern. We estimated the diameter of the QDs to be 4.8 nm by using the Scherrer equation,[22] (K the numerical constant was taken to be 0.93). XPS was used to confirm the presence of Cd^{2+} ($3d_{5/2}$, 405 eV), Se^{2-} (3d, 54 eV), Zn^{2+} ($2p_{3/2}$, 1022 eV), and S^{2-} (2s, 225 eV) in the QDs, as shown in Figure 2. By integrating the areas under the XPS peaks, we estimated the composition of the QDs to be $Cd_{1.2}Se_1Zn_{4.4}S_{5.6}$, which agreed reasonably well with the molar ratio used in the initial solution. Figure 3 shows the HRTEM images of the QDs.

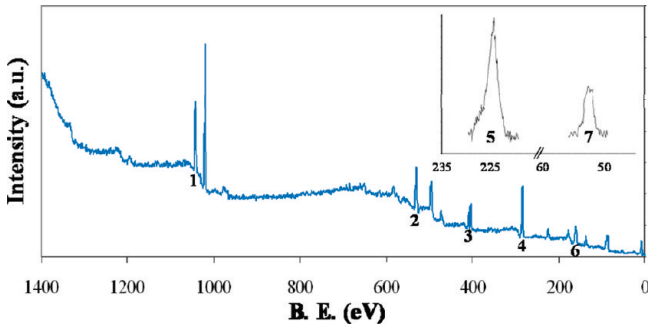

Figure 2. XPS spectrum of the QDs prepared by heating a $Cd_1Se_1Zn_6MPA_{20}$ initial solution at 160 °C for 60 min. 1, Zn 2p; 2, O 1s; 3, Cd 3d; 4, C 1s; 5, S 2s; 6, S 2p; 7, Se 3d. The molar ratio obtained after normalizing the peak areas to Se 3d was calculated as $Cd_{1.2}Se_1Zn_{4.4}S_{5.6}$. For convenience, the S 2s and Se 3d peaks were also expanded in the inset.

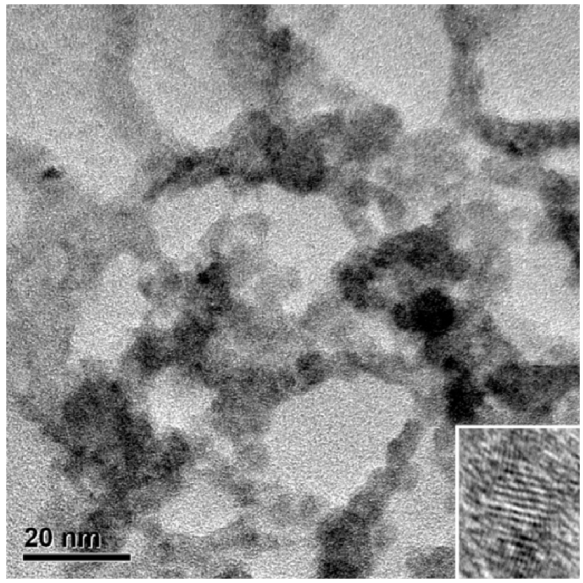

Figure 3. HRTEM images of the QDs prepared by heating a $Cd_1Se_1Zn_6MPA_{20}$ initial solution at 160 °C for 60 min. From high-magnification images (inset), we calculated the average QD diameter as 5.3 nm and confirmed crystallinity and the zinc-blende ZnS structure (111 plane ≈ 3.2 Å).

In the insert, a particle with the lattice fringes are shown, indicating that the QDs were crystalline. Furthermore, we calculated the lattice spacing to be 3.2 Å, which corresponded to the 111 plane of zinc-blende ZnS. The size of the QDs was found to be approximately 5.3 nm in diameter from the high magnification image (estimating the size enclosing the lattice fringes).

Figure 4 shows the influence of postsynthesis UV irradiation. After a 30 min exposure, we measured a 10-fold increase in the I_{maxQD} compared to only a 10% increase in the I_{maxTS}, resulting in a I_{maxQD}/I_{maxTS} of 35 (Table S1, Supporting Information). Additionally, the QD λ_{maxQD} was blue shifted by 11 nm (576 nm → 565 nm). The QD UV−vis absorption spectrum also changed with the characteristic absorption maximum dropping in intensity and broadening toward lower wavelengths (Figure S1, Supporting Information). UV exposure times longer than 30 min did not significantly change the PL characteristics. The relative QY and fwhm of the QDs after 30 min of UV treatment was 22% and 52 nm, respectively.

$Cd_4Se_1Zn_yMPA_{20}$ Initial Solution. The $Cd_1Se_1Zn_6MPA_{20}$ initial solution resulted in highly emissive QDs after postsynthesis UV irradiation. However, our goal was to develop highly

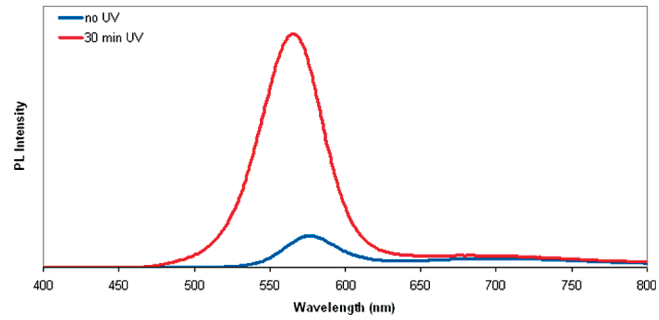

Figure 4. Effect of postsynthesis UV illumination on QDs prepared by heating a $Cd_1Se_1Zn_6MPA_{20}$ initial solution at 160 °C for 60 min. For comparison, the analogous sample not exposed to UV light is also shown. QD solutions were excited at 375 nm.

emissive QDs by using microwave irradiation only. Literature shows that high-quality QDs are typically grown by using a Cd^{2+}/Se^{2-} ratio higher than 1.[15] As such, we examined a series of solutions with $Cd_xSe_1MPA_{20}$ ($x = 1-7$, emission data shown in Table S2, Supporting Information) and chose to optimize the $Cd_4Se_1MPA_{20}$ solution by adding different concentrations of the $Zn(NH_3)_4^{2+}$ complex. These $Cd_4Se_1Zn_yMPA_{20}$ solutions were heated in the microwave oven at 140 °C for 60 min and details of the PL spectra are reported in Table 2. The resulting solutions were stable for months and changed from yellow ($y = 0$) to dark yellow ($y = 4$) in color. At the lowest Zn^{2+} concentration ($y = 1$), we observed a minor blue shift in the λ_{maxQD} when comparing to the analogous sample without Zn^{2+} (517 nm → 511 nm). Additionally, I_{maxQD} and I_{maxTS} increased by 2-fold and 40%, respectively. On adding an excess of Zn^{2+} ($y = 4$), λ_{maxQD} stabilized at 536 nm while I_{maxQD} and I_{maxTS} increased by 7-fold and 3-fold, respectively. These QDs had an I_{maxQD}/I_{maxTS} ratio of 13.8 with relative QY of 4.0% and the fwhm was 60 nm. For comparison, the relative QY of QDs prepared from the $Cd_4Se_1MPA_{20}$ was <1%. After optimizing the microwave heating temperature (150 °C) and time (90 min) for the $Cd_4Se_1Zn_4MPA_{20}$ initial solution (Table 2), the resulting QDs showed a I_{maxQD}/I_{maxTS} ratio of 36, a relative QY of 13%, and a fwhm of 48 nm. Figure 5 shows the UV−vis absorption and PL spectra of these QDs.

We isolated and characterized the QDs that were prepared by heating the $Cd_4Se_1Zn_4MPA_{20}$ solution at 150 °C for 90 min. Figure 6 shows an XRD pattern with three broad peaks in the 20−60° 2θ range, which was comparable to the zinc-blende CdS diffraction pattern. Using the Scherrer equation, we estimated the average diameter of the QDs to be 4.9 nm.[22] Figure 7 shows the XPS and confirms the presence of Cd^{2+} ($3d_{5/2}$, 405 eV), Se^{2-} (3d, 54 eV), Zn^{2+} ($2p_{3/2}$, 1022 eV), and S^{2-} (2s, 225 eV) in the QDs. After integrating the areas under the XPS peaks, we estimated the composition of the QDs to be $Cd_{5.5}Se_1Zn_{3.5}S_{7.6}$, which was similar to the molar ratio used in the initial solution. Also, HRTEM images showed that the QDs were crystalline and approximately 5.0 nm in diameter, as shown in Figure 8. The HRTEM lattice spacing was calculated as 3.4 Å, which was close to the theoretical spacing of the (111) plane of zinc-blende CdS. Using dynamic light scattering, the peak of the hydrodynamic diameter of these QDs was measured as 7 nm (range 5−17 nm).

Biological Imaging. Using the optimized QDs prepared through microwave irradiation ($Cd_4Se_1Zn_4MPA_{20}$ solution heated at 150 °C for 90 min), we utilized laser scanning confocal microscopy to demonstrate their potential for biological labeling. Murine alveolar macrophages readily internalized microwave-synthesized QDs after only 20 min of incubation, while

TABLE 2: Effect of [Zn^{2+}], Microwave Heating Temperature and Time on QDs from $Cd_4Se_1Zn_yMPA_{20}$ Initial Solution[a]

Cd/Se/Zn/MPA	temperature	time	λ_{maxQD}	I_{maxQD}	I_{maxTS}	I_{maxQD}/I_{maxTS}
4:1:0:20	140 °C	60 min	517 nm	2.7×10^6	4.2×10^5	6.4
4:1:1:20	140 °C	60 min	511 nm	5.4×10^6	5.9×10^5	9.2
4:1:2:20	140 °C	60 min	511 nm	1.1×10^7	7.0×10^5	15.7
4:1:3:20	140 °C	60 min	526 nm	1.6×10^7	1.0×10^6	16.0
4:1:4:20	140 °C	60 min	536 nm	1.8×10^7	1.3×10^6	13.8
4:1:4:20	150 °C	60 min	547 nm	3.4×10^7	1.4×10^6	24.3
4:1:4:20	160 °C	60 min	554 nm	8.2×10^6	4.9×10^5	16.7
4:1:4:20	170 °C*	60 min				
4:1:4:20	150 °C	75 min	554 nm	3.9×10^7	1.8×10^6	21.7
4:1:4:20	150 °C	90 min	560 nm	5.7×10^7	1.6×10^6	35.6

[a] QD solutions were excited at 375 nm (* precipitate formed at 170 °C). Cd/Se/Zn/MPA = molar ratio used in initial QD solution; temperature = microwave reaction temperature; time = microwave reaction time; λ_{maxQD} = PL peak QD wavelength; I_{maxQD} = PL peak QD wavelength intensity; I_{maxTS} = peak intensity of QD trap-state emission.

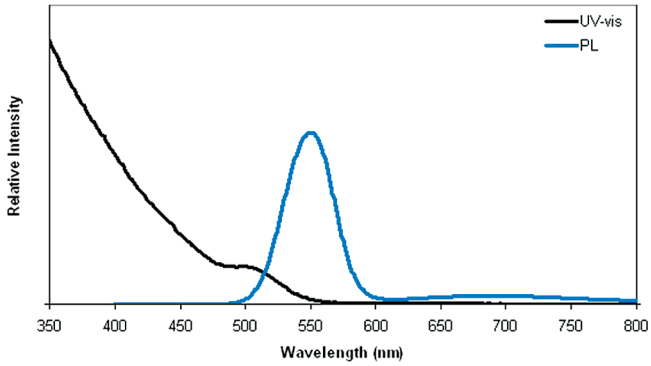

Figure 5. UV−vis absorption and PL spectra of microwave-optimized QDs from a $Cd_4Se_1Zn_yMPA_{20}$ initial solution heated at 150 °C for 90 min. QD solutions were excited at 375 nm.

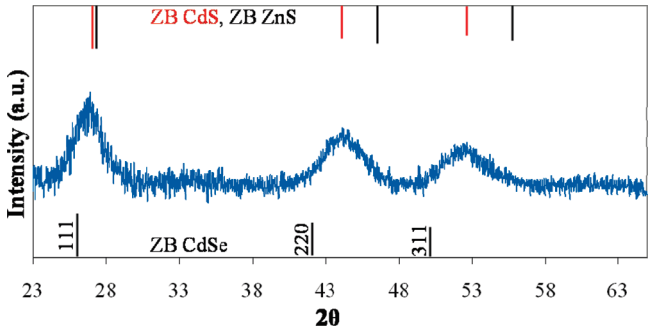

Figure 6. Powder X-ray diffraction pattern of the QDs prepared by heating a $Cd_4Se_1Zn_4MPA_{20}$ initial solution at 150 °C for 90 min. Also shown are the standard diffraction lines for zinc-blende CdSe (below), zinc-blende CdS (above, red), and zinc-blende ZnS (above).

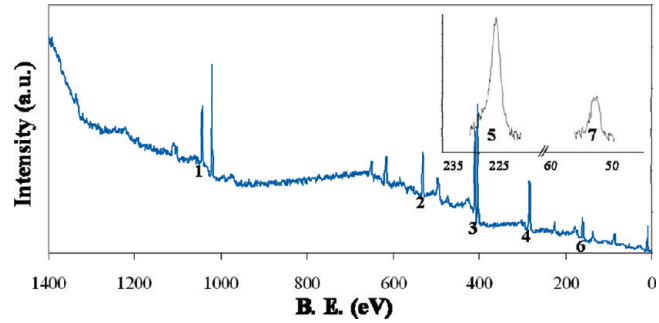

Figure 7. XPS spectrum of the QDs prepared by heating a $Cd_4Se_1Zn_4MPA_{20}$ initial solution at 150 °C for 90 min. 1, Zn 2p; 2, O 1s; 3, Cd 3d; 4, C 1s; 5, S 2s; 6, S 2p; 7, Se 3d. The molar ratio obtained after normalizing the peak areas to Se 3d was calculated as $Cd_{5.5}Se_1Zn_{3.5}S_{7.6}$. For convenience, the S 2s and Se 3d peaks were also expanded in the inset.

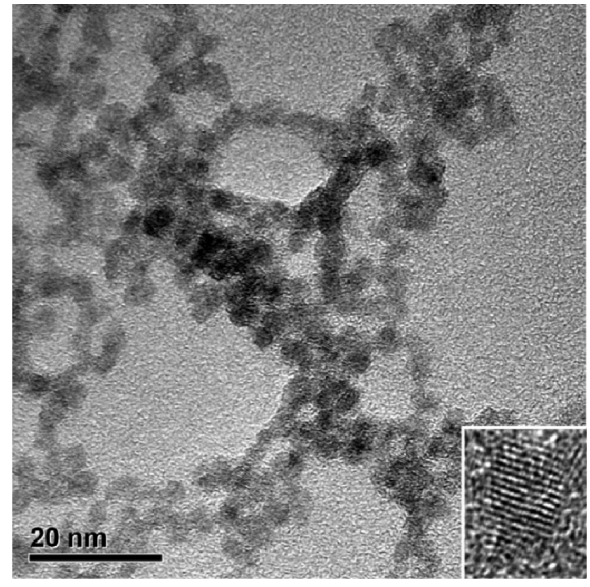

Figure 8. HRTEM images of the QDs prepared by heating a $Cd_4Se_1Zn_4MPA_{20}$ initial solution at 150 °C for 90 min. From high-magnification images (inset), we calculated the average QD diameter as 5.0 nm and confirmed crystallinity and the zinc-blende CdS structure (111 plane ≈ 3.4 Å).

commercial QDot585 QDs were not internalized by this time. Both types of QDs were visible in cells treated with 500, 100, and 20 nM suspensions for 1 h, while no fluorescence was observed in cells treated with 4 nM suspensions. Figure 9 is representative of three independent experiments in which macrophages were treated for 1 h with a 20 nM suspension, the minimum concentration visualized, of either microwave-synthesized or commercial QDot585 QDs. In both cases, the QDs are readily visible within the cells. With the microwaved QD, the cells were also stained with DAPI, a DNA-binding fluorophore that stains cell nuclei. Figure 10 shows that the QDs are primarily localized within the cytoplasm and the nuclear periphery with minimal nuclear penetration.

Discussion

There are currently no microwave procedures in the literature for directly synthesizing aqueous CdSe/ZnS QDs. Multistep methods have been devised, but they almost always rely on a transfer of phase, which can take away from the benefits of microwave irradiation.[23,24] Our direct method used a Zn^{2+} source, $Zn(NH_3)_4^{2+}$, which has not previously been used as a precursor for making CdSe/ZnS-based QDs.

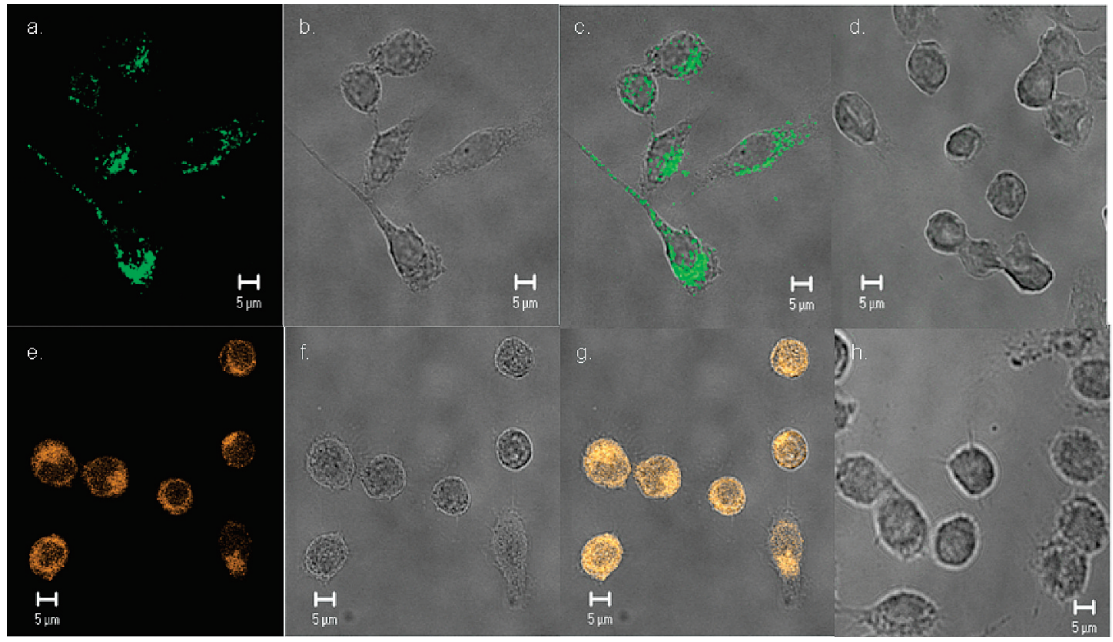

Figure 9. QDs were imaged via confocal scanning microscopy using an excitation wavelength of 488 nm. Murine macrophages treated with 20 nM of microwave-synthesized QDs for 1 h (a−c), and their untreated control (d), versus cells treated with 20 nM suspension of commercial QDot585 (e−g) and their untreated control (h). Fluorescence images (a,e), DIC images (b,f), merged images (c,g), and the negative control merged images (d,h) were acquired. All images were magnified 63× and have a zoom factor of 2.

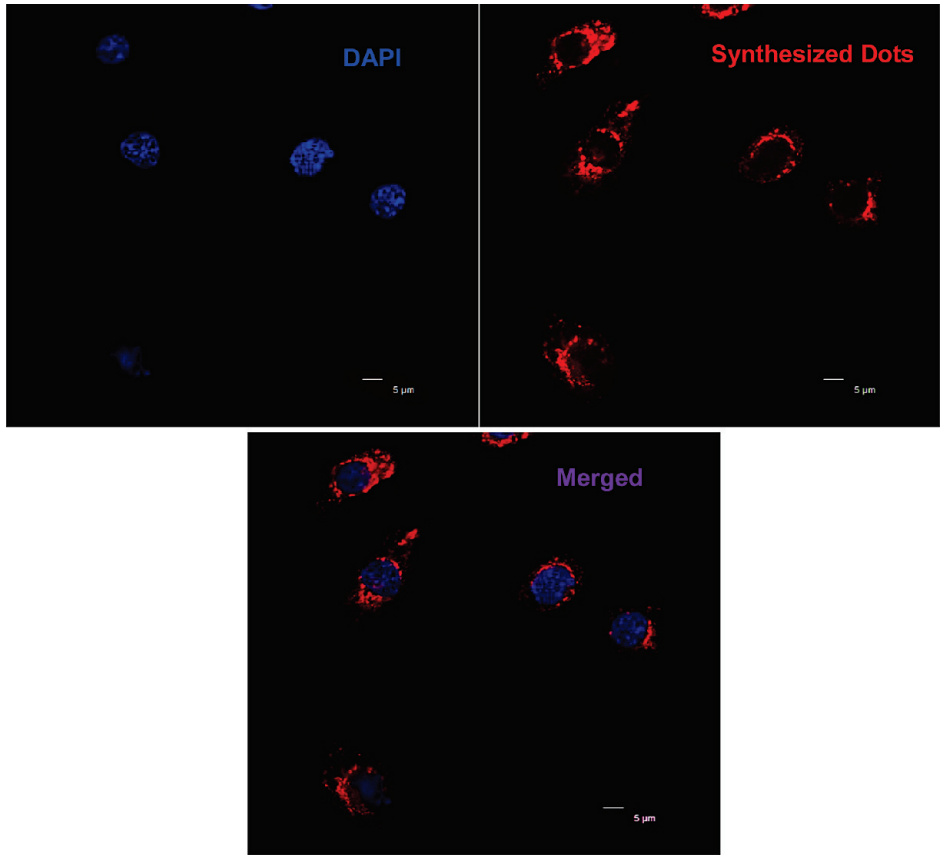

Figure 10. Nuclear exclusion of microwave-synthesized QDs, as evidenced by minimal colocalization in the nuclei of treated cells. Macrophages were treated with a 20 nM suspension of microwave-synthesized QDs for 20 min prior to staining with DAPI. Cells were imaged using scanning laser confocal microscopy with an excitation wavelength of 488 nm (QDs) and 360 nm (DAPI). Magnification is 63× with a zoom factor of 2.

$Cd_1Se_1Zn_yMPA_{20}$ Solutions Lead to QDs with a Poor CdSe/ZnS Interface. We hypothesized that $Cd_1Se_1Zn_yMPA_{20}$ initial solutions would result in CdSe/ZnS core/shell QDs following microwave irradiation. Evidence for this structure can be found in Table 1. I_{maxQD} and I_{maxTS} increased steadily with the Zn^{2+} content, which is consistent with (i) improved passivation of the CdSe core by the ZnS shell (I_{maxQD}) and (ii) increased strain caused by the large lattice mismatch between CdSe and ZnS (I_{maxTS}).[17] Further evidence of the core/shell structure was identified by following λ_{maxQD}, which red shifted

when higher concentrations of Zn^{2+} were added.[17] Had alloy formation occurred, the addition of higher Zn^{2+} concentrations would have resulted in a progressive blue shift of λ_{maxQD}.[25] Despite having several indications that CdSe/ZnS QDs had formed, the low relative QY (≈1.5%) meant that the structure of the QD was not yet optimized. For reference, microwave-synthesized CdSe/CdS QDs typically have a relative QY between 15 and 35%.[15,16,26]

To confirm the structure of QDs synthesized from a $Cd_1Se_1Zn_6MPA_{20}$ initial solution (160 °C for 60 min), we characterized samples by XRD, XPS, and HRTEM. Despite having a λ_{maxQD} in the spectral range of CdSe (576 nm), the XRD pattern was closer to ZnS (Figure 1). As XRD is a bulk measurement, this finding implied the QDs were comprised of a CdSe core encased by a thick ZnS shell. The molar ratio, $Cd_{1.2}Se_1Zn_{4.4}S_{5.6}$, calculated from XPS data further substantiated our claim that these QDs contained primarily ZnS (Figure 2). HRTEM images shown in Figure 3 signified that the QDs were crystalline and approximately 5.3 nm in diameter, which was comparable to the 4.8 nm value predicted by the Scherrer equation. Furthermore, high-magnification HRTEM images show well-defined lattice fringes that extend entirely across the QD with no distinct interface between core and shell. We calculated the lattice spacing to be 3.2 Å, which was close to the 3.13 Å predicted for zinc-blende ZnS. This finding was in agreement with XRD and XPS data since observation of ZnS lattice spacing meant the ZnS shell was thicker than two monolayers.[17]

After exposing the QDs to UV light for 30 min, we measured a 10-fold improvement in the QD I_{max} and an 11 nm blue shift in the QD λ_{max} (Supporting Information, Table S1, Figure 4). Additionally, no significant changes were recorded after 30 min of UV illumination. On the basis of these findings and the prevailing opinions in literature,[27−30] we constructed the following argument to explain the postsynthesis UV light study. Initially, the core/shell interface of the QDs contained many trap-states, as evidenced by the low relative QY of 1.5%. The enhancement upon UV irradiation was caused by photoinduced corrosion of atoms in the presence of dissolved oxygen, of which the net effect was the reduction of defect trap-states caused by lattice mismatch and/or vacancy sites.[30] The large increase in I_{maxQD} (Figure 4) was consistent with the gradual removal of trap-states. This could have been caused by free S^{2-} ions filling Se^{2-} vacancies or direct photoetching of the trap-states themselves. The magnitude of this enhancement (10-fold) was comparable to values reported by Bakalova et al. using similar-sized QDs.[29] With the optimized UV treatment, we could improve the relative QY of our QDs up to 22%, which was similar to the QY of other aqueous QDs prepared by microwave-irradiation.[14−16] However, the UV enhancement process was not practical because it could not be scaled up easily. Therefore, we treated it as a diagnostic tool for characterizing the quality of the core/shell interface of QDs with our conclusion being that the CdSe/ZnS interface was initially poor.

$Cd_4Se_1Zn_yMPA_{20}$ Solutions Lead to QDs with an Improved CdSe/ZnS Interface. We reasoned that the QY of our QDs could be improved by incorporating a layer of CdS between the CdSe and ZnS because its lattice mismatch value is intermediate to CdSe and ZnS.[31] Others have used the same rationale to generate high-quality CdSe QDs.[32] As demonstrated with our previous QD, depositing a ZnS shell directly on the CdSe core QDs led to significant strain, which limited the QY. Alternatively, double shell structures feature incremental changes in lattice spacing, which can relax the overall strain and preserve the QY. Additionally, growth of an outermost ZnS shell can improve biocompatibility and lessen the likelihood of dual-excitation.[17,18] For this type of QD, we chose to optimize the growth conditions of the $Cd_4Se_1MPA_{20}$ initial solution because the resulting QDs displayed a red-shifted $\lambda_{max,QD}$ (Supporting Information, Table S2), indicating formation of the CdS shell.[15]

Because of intrinsic reactivity differences between Cd^{2+} and Zn^{2+}, we concluded that the intermediate CdS layer would form before the outermost ZnS layer.[33] At $y = 4$, λ_{maxQD} red shifted to 536 nm, I_{maxQD} increased by 6-fold, and I_{maxTS} increased by 3-fold (Table 2). These observations are consistent with a ZnS shell being deposited on the CdS intermediate shell. Subsequent optimization of reaction temperature and time (Table 2) led to even greater passivation, and as a result, QDs heated at 150 °C for 90 min generally displayed QY values around 13% and had a I_{maxQD}/I_{maxTS} ratio of about 36.

The powder XRD spectrum shown in Figure 6 was comparable to the zinc-blende CdS pattern, which provided further proof that our modified method resulted in an intermediate CdS layer. XPS data also validated our growth model, as the composition of the QDs now contained more Cd^{2+} than Zn^{2+} ($Cd_{5.5}Se_1Zn_{3.5}S_{7.6}$). Additionally, HRTEM images showed that the QDs were crystalline and approximately 5.0 nm in diameter (Figure 7), which matched well to the diameter estimated by the Scherrer equation, 4.9 nm, but were smaller than the peak 7 nm hydrodynamic diameter obtained from light scattering. The HRTEM lattice spacing was calculated at 3.4 Å, which agreed with the theoretical value for the (111) plane of zinc-blende CdS. This implied that the ZnS layer was less than two monolayers thick and grown coherently.[17]

Performance of Microwave-Synthesized QDs in Biological Imaging. Both microwave-synthesized (from $Cd_4Se_1Zn_4MPA_{20}$ solution) and commercial QDot585 QDs were internalized by macrophages and likely retained in the cytoplasm. A range of concentrations of QDs were tested and suspensions as low as 20 nM were visualized in the cell in case of the microwave-synthesized QD, although the microwave-synthesized QDs appeared to have faster internalization kinetics. The exact mechanisms by which the QDs were internalized are still under investigation. However, Nabiev et al. demonstrated that nonfunctionalized QDs were able to utilize specific cellular transport machinery to travel within cellular compartments, including the nucleus, depending on size and charge.[34] QD size has also been shown to dictate intracellular localization.[35] The peak value of the hydrodynamic diameter of the microwave-synthesized QDs was 7 nm, while the hydrodynamic diameter of the commercial QDot585 QDs was estimated at 15 nm, according to specifications provided by Invitrogen, the supplier of the commercial QDs. Nanoshells coated with polyethylene glycols (PEGs) were not phagocytosed as readily as either negatively- or positively charged core shell nanoparticles.[36] Studies by Clift et al. also found that QDs containing a PEG coating have slower phagocytic kinetics, as compared to carboxyl-containing QDs.[37] As Figure 9 shows, cells exposed to MPA-coated microwave QDs are readily phagocytized and appear to contain punctate aggregates, while cells exposed to PEGylated commercial QDot585 QDs exhibited a more diffuse pattern of fluorescence. Since the size ranges of the two QDs are similar, we hypothesize that the difference in charge between the synthesized and commercial QDs is responsible for apparent differences in their uptake kinetics; however, further investigation will be required to resolve this issue. Figure 10 shows that microwave-synthesized QDs distributed within the cytoplasm with an apparent con-

centration in the perinuclear region with minimal localization in the nucleus, suggesting that their size may prohibit entry into the nucleus through the nuclear pore complexes.[34]

In summary, the microwave-synthesized QDs described here were prepared rapidly and used inexpensive reagents. Postsynthesis UV illumination of QDs prepared from the composition $Cd_1Se_1Zn_6MPA_{20}$ led to improved QD characteristics and led us to the optimal composition of $Cd_4Se_1Zn_4MPA_{20}$ with an intermediate CdS layer between the CdSe and ZnS, which resulted in QDs with 13% QY. These QDs were readily internalized by cells and could be imaged, suggesting promise for use in biological studies.

Acknowledgment. We are grateful to Hendrik Colijn and Lisa Hommel for performing the electron microscopy and XPS work, respectively. We acknowledge funding from the National Science Foundation under Grant 0221678 and NIOSH R01 OH009141.

Supporting Information Available: This material is available free of charge via the Internet at http://pubs.acs.org.

References and Notes

(1) Medintz, I. L.; Uyeda, H. T.; Goldman, E. R.; Mattoussi, H. *Nat. Mater.* **2005**, *4*, 435.
(2) Weng, J.; Ren, J. *Curr. Med. Chem.* **2006**, *13*, 897.
(3) Parak, W. J.; Pellegrino, T.; Plank, C. *Nanotechnology* **2005**, *16*, R9.
(4) Murphy, C. *J. Anal. Chem.* **2002**, *74*, 520A.
(5) Alivisatos, A. P. *Science* **1996**, *271*, 933.
(6) Murray, C. B.; Norris, D. J.; Bawendi, M. G. *J. Am. Chem. Soc.* **1993**, *115*, 8706.
(7) Peng, Z. A.; Peng, X. *J. Am. Chem. Soc.* **2001**, *123*, 183.
(8) Talapin, D. V.; Rogach, A. L.; Mekis, I.; Haubold, S.; Kornowski, A.; Haase, M.; Weller, H. *Colloids Surf.* **2002**, *202*, 145.
(9) Kapitonov, A. M.; Stupak, A. P.; Gaponenko, S. V.; Petrov, E. P.; Rogach, A. L.; Eychmuller, A. *J. Phys. Chem. B* **1999**, *103*, 10109.
(10) Rogach, A. L.; Kornowski, A.; Su, D.; Eychmuller, A.; Weller, H. *J. Phys. Chem. B* **1999**, *103*, 3065.
(11) Zhang, P.; Gao, L. *J. Colloid Interface Sci.* **2004**, *272*, 99.
(12) Kurth, D. G.; Lehmann, P.; Lesser, C. *Chem. Commun.* **2000**, *11*, 949.
(13) Gerbec, J. A.; Magana, D.; Washington, A.; Strouse, G. R. *J. Am. Chem. Soc.* **2005**, *127*, 15791.
(14) Li, L.; Qian, H. F.; Ren, J. C. *Chem. Commun.* **2005**, *4*, 528.
(15) Qian, H.; Li, L.; Ren, J. *Mater. Res. Bull.* **2005**, *40*, 1726.
(16) Qian, H.; Qiu, X.; Li, L.; Ren, J. *J. Phys. Chem. B* **2006**, *110*, 9034.
(17) Dabbousi, R. O.; Rodriguez-Viejo, J.; Mikulec, F. V.; Heine, J. R.; Mattoussi, H.; Ober, R.; Jensen, K. F.; Bawendi, M. G. *J. Phys. Chem. B* **1997**, *101*, 9463.
(18) Derfus, A. M.; Chan, W. C. W.; Bhatia, S. N. *Nano Lett.* **2004**, *4*, 11.
(19) He, Y.; Lu, H.; Sai, L.; Su, Y.; Hu, M.; Fan, C.; Huang, W.; Wang, L. *Adv. Mater.* **2008**, *20*, 3416.
(20) Zhang, H.; Zhou, Z.; Gao, B. M. Y. *J. Phys. Chem. B* **2003**, *107*, 8.
(21) Waldman, W. J.; Knight, D. A.; Huang, E. H.; Sedmak, D. D. *J. Infect. Dis.* **1995**, *171*, 263.
(22) Patterson, A. L. *Phys. Rev.* **1939**, *56*, 978.
(23) Ziegler, J.; Merkulov, A.; Grabolle, M.; Resch-Genger, U.; Nann, T. *Langmuir* **2007**, *23*, 7751.
(24) Roy, M. D.; Herzing, A. A.; De Paoli Lacerda, S. H.; Becker, M. L. *Chem. Commun.* **2008**, *18*, 2106.
(25) Zhong, X.; Han, M.; Dong, Z.; White, T. J.; Knoll, W. *J. Am. Chem. Soc.* **2003**, *125*, 8589.
(26) Hines, M. A.; Guyot-Sionnest, P. *J. Phys. Chem.* **1996**, *100*, 468.
(27) Shavel, A.; Gaponik, N.; Eychmuller, A. *J. Phys. Chem. B* **2004**, *108*, 5905.
(28) Lin, Y.; Hsieh, M.; Liu, C.; Chang, H. *Langmuir* **2005**, *21*, 728.
(29) Bakalova, R.; Zhelev, Z.; Jose, R.; Nagase, T.; Ohba, H.; Ishikawa, M.; Baba, Y. *J. Nanosci. Nanotechnol.* **2005**, *5*, 887.
(30) Torimoto, T.; Nishiyama, H.; Sakata, T.; Mori, H.; Yoneyama, H. *J. Electrochem. Soc.* **1998**, *145*, 1964.
(31) Xie, R.; Kolb, U.; Li, J.; Basche, T.; Mews, A. *J. Am. Chem. Soc.* **2005**, *127*, 7480.
(32) Talapin, D. V.; Mekis, I.; Gotzinger, S.; Kornowski, A.; Benson, O.; Weller, H. *J. Phys. Chem. B* **2004**, *108*, 18826.
(33) Ge, J. P.; Xu, S.; Zhuang, J.; Wang, X.; Peng, Q.; Li, Y. D. *Inorg. Chem.* **2006**, *128*, 4922.
(34) Nabiev, I.; Mitchell, S.; Davies, A.; Williams, Y.; Kelleher, D.; Moore, R.; Gun'ko, Y. K.; Byrne, S.; Rakovich, Y. P.; Donegan, J. F.; Sukhanova, A.; Conroy, J.; Cottell, D.; Gaponik, N.; Rogach, A.; Volkov, Y. *Nano Lett.* **2007**, *11*, 3452.
(35) Ryman-Rasmussen, J. P.; Riviere, J. E.; Monteiro-Riviere, N. A. *J. Invest. Dermatol.* **2007**, *1*, 143.
(36) Zahr, A. S.; Davis, C. A.; Pishko, M. V. *Langmuir* **2006**, *19*, 8178.
(37) Clift, M. J. D.; Rothen-Rutishauser, B.; Brown, D. M.; Duffin, R.; Donalson, K.; Proudfoot, L.; Guy, K.; Stone, V. *Toxicol. Appl. Pharmacol.* **2008**, *3*, 418.

JP901003R